Labor Induction failure prediction using Gabor filterbanks and Center Symmetric Local Binary Patterns

Pablo Vásquez Obando *†, Nestor Arana A. †, Alberto Izaguirre †, and Jorge Burgos ‡
* Faculty of Eletrical and Computer Engineering
National University of Engineering, Managua,Nicaragua
Email: pablo.vasquez@uni.edu.ni
‡ Obstetrics and Gynecology Service
BioCruces Health Research Institute, Bilbao, Spain
† Mondragon University, Basque Country, Spain
Email: narana,aizagirre@mondragon.edu

Abstract—Labor induction is defined as the artificial stimulation of uterine contractions aimed to induce vaginal birth. Occurring in about 20% of pregnancies labor induction has become one the most commonly practiced procedures in obstetrics. One of the risk related to labor induction is cesarean section which accounts about 20% of the inductions. A requirement for a successful labor is a ripe cervix (soft and distensible) . Microestructural changes occurring in the cervix during the ripening process, will affect the interaction between cervical tissues and sound waves during ultrasound transvaginal scanning and will be perceived as gray level intensity variations in the echographic image. A non-invasive method using image processing of ultrasound images may help in predicting the outcome of labor induction. In this paper a set of echography images from labor induction patients is analyzed using a multiscale methodology based on Center Symmetric Local Binary Patterns and Gabor filters. Results show that it is feasible to predict the outcome of a labor induction procedure using this method with a good accuracy

I. Introduction

Nowadays labor induction has become one of the most performed obstetric procedures. Labor induction is indicated when the maternal or fetal benefits from delivery outweigh the risks of prolonging the pregnancy. Indications for induction vary in severity and may be for medical, obstetrical or elective reasons. Some risks related to labor induction are: cesarean section, intrapartum fetal heart rate alterations, infections, fetal acidosis, and postpartum hemorrhage. Currently in Spain about 30% of deliveries are induced and about 20% [7] end in cesarean section. Some of these unwanted outcomes results from intervening when the uterus and cervix are not ready for labor. For this reason, the evaluation of cervical ripening is a crucial step when planning a labor induction procedure

II. Patients and Data

The database used in this paper consist of images from patients admitted for labor induction procedures at the Obstetrics and Gynecology Service, Biocruces Health Research Institute (Bilbao, Spain) during a period of one year. The inclusion criteria were singleton pregnancies, and $\geqq 37$ weeks of gestation. Pregnancies of fetus suffering from infections and abnormalities were not included.

TABLE I
The database used in our experiments.

Category	Samples	Total
Vaginal delivery	212	212
Cesarean Section		31
dilatation stopping	21	
induction failure	10	
Total		243

Annotations about weeks of pregnancy, labor induction indication and outcome were also attached to the collected images. Settings for the ultrasound scanner were defined in a protocol and practiced for all obstetricians participating in this study. Images were acquired during routine patient transvaginal scanning prior to labor induction. All images were acquired as DICOM files but pixel information was extracted as bitmaps for further processing.

The labor induction process has been divided into two stages: A 24 hours ripening stage where prostaglandins are administered, followed by an additional 12 hours stimulation stage where the treatment is changed to oxytocin in case cervical ripening is not achieved. A successful ripening is thus defined when a vaginal delivery was obtained within 24 hours after induction is started. Labor induction failure is considered when after 36 hours the cervix still has a Bishop Score ≤ 6.

All images were acquired with a Voluson E8 Ultrasound scanner from General Electric. A total of 243 DICOM files were acquired, and from these 60 belong to patients with a vaginal delivery and 22 to cesarean section as detailed in table I.

Two ROIs were included with each image. These ROIs were manually delineated by an expert obstetrician and defined several regions in the cervix lips as described in figure 1. The motivation for including these ROIs was to

study if there is an optimal lip region for texture analysis as it has been found in similar texture analysis.

III. Theoretical background

Extracting useful information from Ultrasound (US) B-mode images is a challenging task. US images are low contrast, contain blurred edges and they are normally contaminated with speckle noise. Despite these drawbacks a lot of effort has been made on processing US images.

The objective of this research was to study the feasibility of constructing texture-based reliable algorithms for predicting labor induction outcome. One important aspect of texture is scale. It is known that the human visual system processes images in a multi-scale way. There are many neurophysiological and psychophysical data indicating the multiscale analysis by the human visual front-end system [10]. The visual cortex has separate cells that respond to different frequencies and orientations. Analyzing texture at several resolutions is required when dealing with non-stationary textures as those obtained in medical imaging. We resort to a Gabor filter bank to analyse the images in our database.

A. The Gabor filter

Gabor filters are constructed by combining oriented complex sinusoidal modulated by Gaussians functions. Gabor filtering has emerged as one of the leading approaches. The capability of texture discrimination of Gabor functions seems to be related both to their optimal joint resolution in space and frequency, and to their aptitude of modeling the response of cortical cells (simple cells) devoted to the processing of visual signals. The link between Gabor functions and the visual system of mammals has been investigated and discussed by various authors.

Although Gabor filters are widely adopted, they suffer from certain limitations, mainly because they depend on various parameters that need to be set properly. This problem, sometimes referred to as filter bank design, involves the selection of a suitable number of filters at different orientations and frequencies.

These filters have been used extensively in image processing applications such as texture segmentation [1, 2, 12], image retrieval [13] and texture classification [3, 5]. It performs a localized and oriented frequency analysis of a two-dimensional signal. The formulation in the spatial domain is as follows:

$$g(x,y) = \frac{1}{2\pi\sigma_x\sigma_y}\exp\left[-\frac{1}{2}\left(\frac{\tilde{x}^2}{\sigma_x^2}+\frac{\tilde{y}^2}{\sigma_y^2}\right)\right]\exp\left(2\pi jW\tilde{x}\right) \quad (1)$$

$$\begin{cases}\tilde{x} &= x\cos\theta + y\sin\theta\\ \tilde{y} &= -x\sin\theta + y\cos\theta\end{cases} \quad (2)$$

Where σ_x and σ_y characterize the spatial extent and bandwidth of the filter, and w_X is the modulation frequency. θ ($\theta \in [0,\pi)$) specifies the orientation of the filter. W is is the radial frequency of the sinusoid. The Fourier transform of the Gabor function en equation 1 is given by:

$$G(u,v) = \exp\left[-\frac{\pi^2}{F^2}\left(\gamma^2(\tilde{u}-W)^2+\eta^2\tilde{v}^2\right)\right] \quad (3)$$

$$\begin{cases}\tilde{u} &= u\cos\theta + v\sin\theta\\ \tilde{v} &= -u\sin\theta + v\cos\theta\end{cases} \quad (4)$$

where $\gamma = 2\pi\sigma_x$, $\eta = 2\pi\sigma_y$. The Fourier representation in equation 3 specifies the amount by which the filter modifies each frequency component of the input image.

1) Gabor filter bank.: The design of a filter bank consist of a proper set of values for the filter parameters. Choosing optimum parameters for the filter bank is not a trivial task. By optimum, it is meant the ones providing the highest texture discriminating features. Due the many variables involved in the selection the search space is usually big. For this reason a complete search it is not advisable and some heuristics are necessary. Some good methods to cope with this problem are based on genetic algorithms [6] or simulated annealing (ISA) [11]. In this work the artificial bee colony algorithm is used to find optimal or nearly optimal set of parameters.

The design of the filter bank involves the use of the following expressions to calculate the main parameters :F, η, γ, B_f, B_t.

$$\gamma = \frac{1}{\pi}\left(\frac{2^{B_f}+1}{2^{B_f}-1}\right)\sqrt{B_f\ln 2} \quad (5)$$

$$\eta = \frac{1}{\pi}\left(\frac{\sqrt{B_f\ln 2}}{\tan\left(\frac{B_t}{2}\right)}\right) \quad (6)$$

$$F_i = 2^{iB_f}F_0 \quad (7)$$

where B_f is the filter bandwidth in octaves, $B_t = \frac{2\pi}{N}$ is the angular spacing between different filters (N is the number of different orientations) and F_0 is the minimum normalized frequency to be considered during analysis, the maximum frequency is usually set as 0.4 or 0.5.

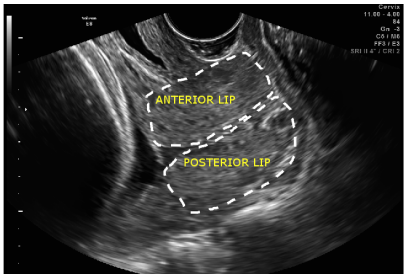

Fig. 1. A sample TVU image showing the two ROIS corresponding to the anterior and posterior cervical lips.

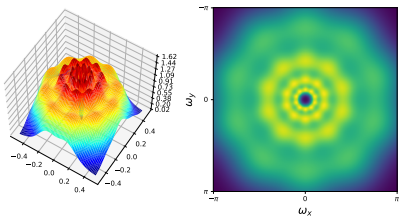

Fig. 2. An example of a Gabor filter bank frequency partitioning. Parameters for the filters are: $N = 12$, $F_0 = 0.05$,$F_{max} = 0.5$ and $B_f = 1$

Parameters η and γ are the same in equation 3. All of these parameters are chosen in such a way that the filter bank cover all the frequency domain. An example of this frequency partitioning performed by a filter bank can be observed in figure 2.

B. The Center Symmetric Local Binary Pattern (CS-LBP)

The center symmetric local binary pattern is another modification of the original LBP descriptor [4]. The original implementation of LBP produced very long histograms and its feature is not robust on flat images. In CS-LBP instead of comparing the gray level value of each pixel with the center pixel, the center symmetric pairs of pixels are compared, see figure 3. CS-LBP is closely related to gradient operator. It considers the grey level differences between pairs of opposite pixels in a neighborhood. So CS-LBP take advantage of both LBP and gradient based features. It also captures the edges and the salient textures and it is less affected by noise.

To increase the operator's robustness in flat areas, the differences are thresholded at a typically non-zero threshold T. The histogram of CS-LBP values for an image I is stored as its feature. Three parameters have to be set during CS-LBP analysis: radius R, number of neighboring pixels N, and threshold on the gray level difference T.

C. The Artificial Bee Colony Algorithm (ABC)

The artificial bee colony algorithm is an example of the swarm intelligence algorithm class. It was proposed by Pham [9] and try to imitate the food foraging behavior

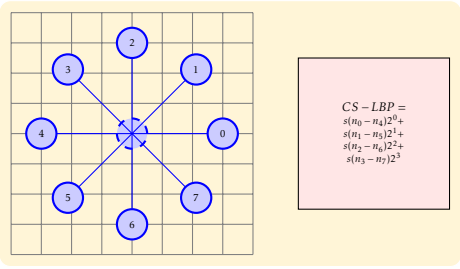

Fig. 3. Example of CS-LBP feature calculation for a neighborhood $P = 8$ and radius $R = 1$. The n_i denotes the i^{th} neighbor and $s()$ is a thresholding operation.

of swarms of honey bees. According to their authors ABC is applicable to both combinatorial and functional optimization problems. In ABC there exist three types of bees: employed bees, onlookers and scouts. ABC process requires cycle of four phases: initialization phase, employed bees phase, onlooker bees phase and scout bee phase.

Employed bees search food in the vicinity of the food source stored in their memory. They share food information with onlooker bees which tend to select food sources from those found by the employed bees. The source with the highest fitness (quality) is assigned a higher probability to be selected by the onlooker bees than others with lower quality. Scout bees are translated from a few employed bees, which abandoned their food sources after a predefined number of attempts and search now ones.

In the ABC algorithm, the first half of the swarm consists of employed bees, and the second half constitutes the onlooker bees. The number of employed bees or the onlooker bees is equal to the number of solutigons in the swarm

During initialization, a randomly distributed initial population of SN solutions (food sources) is generated (equation 8), where SN denotes the swarm size. Each solution $x_i (i = 1, 2, ..., SN)$ is a D-dimensional vector, where D is the number of variables in the optimization problem and x_i represents theth food source in the population.

$$x_i^j = x_{min}^j + rand(0,1)(x_{max}^j - x_{min}^j), \forall_j = 1, 2.., D \quad (8)$$

$$v_{i,j} = x_{i,j} + \phi_{i,j}(x_{i,j} - x_{k,j}) \quad (9)$$

$$p_i = \frac{fit_i}{\sum_{i=1}^{SN} fit_i} \quad (10)$$

$$x_i^j = x_{min}^j + rand[0,1](x_{max}^j - x_{min}^j), \forall_j = 1, 2.., D \quad (11)$$

Each employed bee generates a new candidate solution in the neighborhood of its present position (equation 9) where $x_{k,j}$ is a randomly selected candidate $(i \neq k)$ solution k, is a random dimension index selected from the set, and $\phi_{i,j}$ is a random number within [-1,1].

After the new candidate solution $v_{i,j}$ is generated its fitness is checked, if its value is higher than of its parent x_i^j then update it with $v_{i,j}$ otherwise keep the current value.

Once all employed bees complete the search process, they share the information of their food sources with the onlooker bees. An onlooker bee evaluates the nectar information taken from all employed bees and chooses a food source with a probability related to its nectar amount. This probabilistic selection is really a roulette wheel mechanism (equation 10), where fit_i is the fitness value of the i^{th} solution in the swarm,we use $fit = e^{\frac{-c_i}{\bar{c}}}$, with c_i as the current cost and $\bar{c}$ is the average cost among all solutions.

As seen, the better the solution i, the higher the probability of the i^{th}food source selected. If a position

cannot be improved over a predefined number (called limit) of cycles, then the food source is abandoned. Assume that the abandoned source is x_i, then the scout bee discovers a new food source using equation 11 where and x^j_{min} and x^j_{max} are lower and upper boundaries of the jth dimension, respectively.

Since the ABC algorithm was developed for optimization of continuous functions it has been modified to work with discrete type values. In particular equations 8, 9, 11 have the form:

$$k^j = randint(0, N_j) \tag{12}$$

$$x^j_i = x[k^j] \tag{13}$$

$$v_{i,j} = x_{i,j} + round(a_j \phi_{i,j}(x_{i,j} - x_{k,j})) \tag{14}$$

Where N_j is the number of different discrete values of each variable. a_j controls de displacement of the variable. If the displacement goes beyond maximum values in each variable range then the maximum value is used.

IV. Image Processing

Images in the database are rather big (975 x375 pixels) and some areas do not contain relevant information such as annotations and dark areas resulting from scan conversion and not corresponding to sector scanning. For this reason a squared area of $600x600$ pixels containing our regions of interest were cropped from every image and the ROI coordinates were also transformed for their use in the smaller images.

The images were normalized to have zero mean and unit variance. This is needed since we don't want the DC component to be present when performing convolution. The images included two ROIs corresponding the anterior (ANT) and posterior (POST) regions.

The filter bank with the optimal parameters was used for decomposing the images into $k * N$ different components where $k = \frac{1}{B_f} \log_2 \left(\frac{F_{max}}{F_0} \right)$. Every component is then processed using the CS-LBP.

A binary mask constructed from the defined ROIs was applied to each processed component to select only the points inside the ROIs. With the obtained pixels a histogram of 2^{np} bins is created. $np = \frac{P}{2}$ is the number of pixel pairs used. As we used $P = 8$ neighbors for CS-LBP analysis then the obtained histograms are 16 bins long $(2^{\frac{8}{2}})$.

A. Optimum values for our filter bank

The modified ABC algorithm was used to find optimal or nearly optimal set of parameters for our Gabor filter bank. The search space is described in table II.

The cost function utilized was the distance between two model (vectors) representing each category (cesarean, vaginal). These vectors are actually the average of histograms calculated using the concatenated CS-LBP texture descriptor histograms at each scale and orientation and for each ROI (ANT,POST). The distance metric used in the calculation was histogram intersection. Vector a_j was set to $a_j = [1, 0.5, 0.0, 0.5, 0.2]$. Using this methodology, the optimum values found are : $N = 14$, $B_f = 0.5$, $F_0 = 0.05$, $F_{max} = 0.35$, $T = 0.05$.

TABLE II
Parameter search space.

Parameter	Values
N	4 , 6, 8, 10, 12,14
B_f	0.5, 0.75, 1, 1.25, 1.5
F_0	0.05, 0.10, 0.15, 0.2, 0.25
F_{max}	0.35, 0.40, 0.45, 0.5
T	0.01, 0.02, 0.03, 0.05, 0.10

B. Classification

As obtained vectors were rather high-dimensional, a feature selection step was introduced before feeding data into classifiers. Only the best 100 features were selected and sent to a support vector machine classifier with a radial basis functions kernel, using a regularization parameter $C = 0.9$. A receiving operating curve (ROC) is used to evaluate system performance. A ROC is a plot of genuine acceptance rate against false acceptance rate. Points in this curve belong to all possible system operating states. The resulting ROC curve is shown figure 4.

V. Discussion

In this paper a multi-scale Center Symmetric Local Binary Pattern methodology for the problem of assessing cervical ripening is proposed. Performing texture analysis of ultrasound images is not a trivial task; the difference between images corresponding to the two different outcomes (vaginal and cesarean) are not distinguishable to the bare eye.

Parameters for the design of our filter bank were obtained using swarm-intelligence-based methods that helps in reducing the time spent on finding appropriate values for these parameters. ABC algorithm proved to be useful for this task. By using information from different frequency bands and orientations, an improvement in

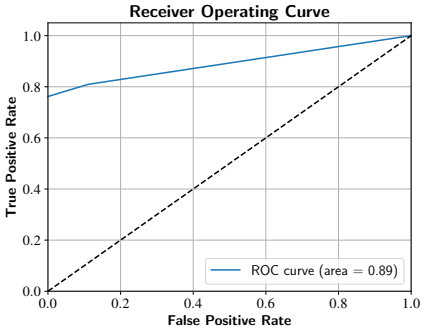

Fig. 4. ROC curve obtained

accuracy of prediction is achieved compared to previous texture approaches [8] based on local descriptors only.

Our results show that it is possible to differentiate, by means of image processing techniques, a ripe cervix and therefore the type of outcome from labor induction, with an accuracy of about 84 %.

References

[1] Chung Ming Chen, H. H S Lu, and Ko Chung Han. "A textural approach based on gabor functions for texture edge detection in ultrasound images". In: Ultrasound in Medicine and Biology 27.4 (2001), pp. 515–534. issn: 03015629.

[2] I. Fogel and D. Sagi. "Gabor filters as texture discriminator". In: Biological Cybernetics 61.2 (1989), pp. 103–113. issn: 03401200.

[3] G.M. Haley and B.S. Manjunath. "Rotation-invariant texture classification using modified Gabor filters". In: Proceedings., International Conference on Image Processing 1 (1995), pp. 262–265.

[4] M Heikkilä, M Pietikäinen, and C Schmid. "Description of interest regions with center-symmetric local binary patterns". In: Computer Vision, Graphics and Image Processing. 2 (2006), pp. 58–69. issn: 00313203.

[5] Mahamadou Idrissa and Marc Acheroy. "Texture classification using Gabor filters". In: Pattern Recognition Letters 23.9 (2002), pp. 1095–1102. issn: 01678655.

[6] Ma Li and R. C. Staunton. "Optimum Gabor filter design and local binary patterns for texture segmentation". In: Pattern Recognition Letters 29.5 (2008), pp. 664–672. issn: 01678655.

[7] Francisca S. Molina and Kypros H. Nicolaides. "Ultrasound in labor and delivery". In: Fetal Diagnosis and Therapy 27.2 (2010), pp. 61–67. issn: 10153837.

[8] Pablo Vásquez Obando et al. "Multiscale Texture Analysis of Cervical Tissue for Labor Induction". In: 2015 IEEE International Workshop of Electronics, Control, Measurement, Signals and their application to Mechatronics. 2015.

[9] D.T. Pham et al. "The bees algorithm–A novel tool for complex optimisation". In: Proceedings of the 2nd International Virtual Conference on Intelligent Production Machines and Systems (2006), pp. 454–459.

[10] Bart M. Haar Romeny. Front-End Vision and Multi-Scale Image Analysis: Multi-scale Computer Vision Theory and Applications, Written in Mathematica. 2003, p. 470. isbn: 9781402015038.

[11] Du-Ming Tsai, Song-Kuaw Wu, and Mu-Chen Chen. "Optimal Gabor filter design for texture segmentation using stochastic optimization". In: Image and Vision Computing 19.5 (2001), pp. 299–316. issn: 02628856.

[12] T.P. Weldon and W.E. Higgins. "Design of multiple Gabor filters for texture segmentation". In: 1996 IEEE International Conference on Acoustics, Speech, and Signal Processing Conference Proceedings 4.4 (1996), pp. 2243–2246. issn: 1520-6149.

[13] Dengsheng Zhang et al. "Content-based Image Retrieval Using Gabor Texture Features". In: IEEE Transactions PAMI 3656 LNCS (2000), pp. 13–15. issn: 03029743.